Millimeter Waves for Short-Range Multimedia Communication Systems

ORESTE ANDRISANO, MEMBER, IEEE, VELIO TRALLI, MEMBER, IEEE, AND ROBERTO VERDONE, MEMBER, IEEE

A framework for performance characterization of short-range communications systems is developed with the intention of investigating the feasibility of new multimedia wireless services at millimeter waves (MMW's). Both narrow- and wide-band systems are considered for mobile and/or fixed users. This paper aims at defining and evaluating proper metrics to characterize the service quality for the user and jointly takes the propagation characteristics, the transmission techniques, and the multiple access protocols into account. The definition of service-oriented metrics is emphasized.

Three different real scenarios operating at MMW are investigated with a unified perspective: intelligent transport systems, wide-band local-area networks, and local multipoint distribution systems for interactive video services. The role played by the MMW band in the development of these services is discussed.

In each scenario, accurate propagation analysis is carried out and suitable countermeasure techniques are pointed out in order to join suitable service-quality levels. The methodology considered is based on both analytical and semianalytical tools for performance evaluation.

Keywords*— *Millimeter waves, multimedia, performance, wireless.

I. INTRODUCTION

In the last decade, several efforts have been dedicated to the investigation of wireless communication systems able to provide interactive and multimedia services to users in different contexts, such as, e.g., the mobile (indoor, urban, suburban, highway) environment. Due to spectrum congestion (and other reasons, as will be explained in this paper), the interest of researchers and standardization bodies has indicated the millimeter wave (MMW) band as a candidate for some of the most challenging services to be provided in the next decade (see, e.g., [1]–[18]).

Hence, some works have been presented to describe the wireless channel behavior at those frequencies, such as the 60–64-GHz band, where propagation is characterized by high levels of attenuation due to rain and oxygen absorption, or the 30- and 40-GHz bands, where some broad-band video services are proposed to be operating in the future [19]–[25]. Some of these works have been developed within the context of various European projects, such as DRIVE, PROMETHEUS, and MBS [2], [26]–[28].

On the other hand, the use of the MMW band (and, particularly, of the 60–64-GHz band) introduces some features that have to be taken into account in system design; these features are mainly related to the short wavelength and to the additional attenuation due to rain and oxygen absorption, when present. The former requires appropriate methods of performance estimation: more precisely, the choice of the performance metrics and, as a consequence, of the quality requirements has to be thoroughly discussed, also in conjunction with the kind of service provided, leading to the definition of service-oriented metrics. Section IV of this paper is devoted to this topic. The topic introduces some effects on interference control and cell planning, as will be shown in Section V.

In this paper, a discussion on the design criteria of communications systems at MMW's is given, and performance evaluation is carried out. Three different kinds of systems that are expected to be available in the next few years, probably by making use of the advantages of the MMW band, are introduced and investigated: intelligent transport systems, wireless local-area networks, and local multipoint distribution systems.

The aim of this paper is to give a unified description of design methods and criteria and to show how these methods can be applied to the three systems considered. The numerical results will show the main guidelines of the communication systems design at MMW.

The structure of this paper is the following. Section II describes the three services considered and gives motivation for the use of MMW band. Section III introduces the structure of the transmission system under a unified approach. In Section IV, the performance characterization criteria are explained; this section represents the core contribution

Manuscript received January 16, 1998. This work was supported by a contract from the Consiglio Nazionale delle Richerche, Bologna, Italy.

The authors are with the Centro di Studio per l'Informatica e i Sistemi di Telecomunicazioni—Consiglio Nazionale delle Richerche, University of Bologna, DEIS, Bologna 40136 Italy.

Publisher Item Identifier S 0018-9219(98)04239-X.

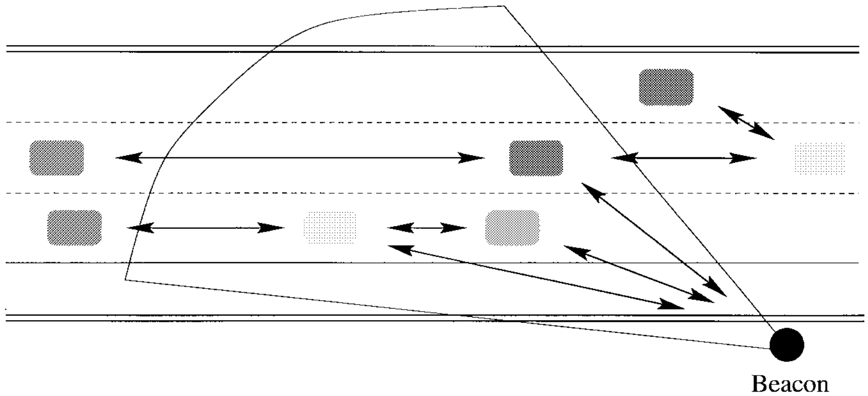

Fig. 1. IVC and RVC in the context of an ITS application (highway scenario).

of this paper, together with the numerical evaluations described in the following sections.

II. Why Millimeter Waves?

The main advantages of the use of MMW's can be summarized as follows:

i) the high power level attenuation, due to the large value of frequency, in conjunction with oxygen and rain absorption (in the 60–64-GHz band), which leads to a high spatial filtering effect with the consequent frequent channel reuse;

ii) the small size of antennas and radio-frequency (RF) circuits;

iii) the large spectrum availability.

On the other hand, large values of signal attenuation become a fundamental drawback when long-distance communication links are to be managed. Hence, significant applications of the MMW can be found in the field of short-range communication systems, that is, when link distances range from a few meters up to one kilometer.

Another useful consequence of the MMW band utilization, related to the large values of attenuation, is the low number of interfering signal sources that are usually present in the system. Both in indoor environments, due to walls, and in outdoor scenarios, due to high frequency (and the use of directive antennas), a number of interferers ranging from zero to two or three may be present [29]–[32]. This represents a significant advantage in terms of capture probability when packet communications and narrow-band signaling are considered.

Several applications of the MMW band are envisaged for future services that will characterize the end of this century and/or the beginning of the next one.

In this paper, we cover three different application areas that could take advantage of use of the MMW band:

1) intelligent transport systems (ITS's);
2) wireless local-area networks (WLAN's) for multimedia applications;
3) local multipoint distribution systems (LMDS's) for interactive video services.

A brief description of the three kinds of applications is given, and the advantages [items i), ii), iii)] exploited by each of them are indicated.

A. ITS's

ITS's use information, transport, and communications technologies, in vehicles as well as within the infrastructure, to improve mobility while increasing transport safety, reducing traffic congestion, maximizing comfort, and reducing environmental impact.[1]

In recent years, particular attention has been paid to wireless short-range systems for intervehicle and roadside-to-vehicle communications (IVC and RVC, respectively), aiming at improving the safety and efficiency of traffic flow in different areas, such as urban environments and highways [33]–[43].

The role of the RVC network is that of supplying the user (the driver) with information related to weather forecasts, on a small and a large scale, parking availability, traffic conditions, etc. The IVC network, on the other hand, aims at allowing a direct exchange between vehicles of messages related to their position, speed, acceleration, and emergency situations (presence of fog, ice on the ground, accidents, etc.); hence, it could support the driver with local information even in the absence of the fixed infrastructure.

If a communication system able to allow both IVC and RVC is to be defined (see Fig. 1), it is convenient to investigate a common standard protocol. In both cases, a packetized access to the medium is normally considered [33]. Different frequency ranges have been investigated or recommended for these systems, mainly the 5.8-GHz [33], 63.5-GHz [43], and infrared bands [1]. Since IVC systems need short-range links to be exploited, due to the local significance of the information exchanged (position, speed, acceleration, presence of ice on the ground, etc.), the 63.5-GHz band has some advantages with respect to 5.8 GHz. In fact, also due to oxygen absorption in the 60–64-GHz frequency range (with specific attenuation $\alpha_{ox} \approx 9$ dB/Km

[1] See http://www.ertico.com.

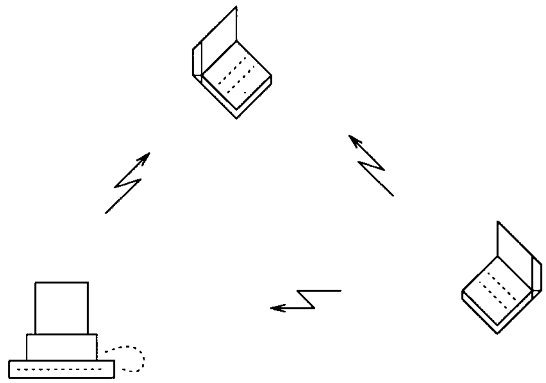

Fig. 2. WLAN scenario.

at 63.5 GHz), a higher degree of spatial filtering can be obtained by using this bandwidth with respect to 5.8 GHz [item i)]. On the other hand, unlike infrared systems, by means of multipath propagation a communication link may exist at MMW even in nonline-of-sight (NLOS) conditions. Moreover, the small size of antennas and RF circuits is of great interest since these components should be integrated (and hidden) in the structure of cars [item ii)]. For these reasons, the 63.5-GHz band is a strong candidate for the evolution of IVC and RVC systems for ITS applications. In both cases, by considering safety and/or congestion control, data rates are on the order of a few megabits per second [4], [42], [43].

B. WLAN

Within the context of multimedia communications, increasing attention to WLAN's is expected in the next few years. The benefits that WLAN's can offer to the end user mainly consist of mobility and installation flexibility with respect to fixed LAN's [44]–[47] (see Fig. 2). More precisely, the demand of wide-band multimedia services arising from wireless users has stimulated particular interest in the design of high-quality, high-speed (beyond 10 Mbit/s, up to 155 Mbit/s), wireless networks able to provide access to services and capabilities of broad-band fixed networks. These networks are mainly devoted to short-range coverage, as in the case of WLAN in indoor environments. To support integrated broad-band communications, wireless asynchronous transfer mode (ATM) will play an important role [48], [49].

Recently, some studies and proposals concerning high-speed transmission systems for WLAN and wireless ATM have appeared in literature. In [5] and [6], 150–155-Mbit/s systems for packet transmission in an indoor environment based on coded orthogonal frequency division multiplexing (OFDM) have been proposed, whereas in [50], a clustered coded OFDM with transmitter diversity is considered to reduce the effects of nonlinear power amplifiers and to introduce space diversity. In [51], on the other hand, the possibility of using equalization is discussed, and some efficient structures are proposed. In this context, we focus on coded OFDM for high-speed transmission, and we investigate system behavior in an actual indoor scenario [7].

As broad-band radio requires large bandwidth availability, less congested bands (e.g., 60 GHz) recently have been investigated [19]–[23]. Hence, the large spectrum availability of the MMW band [item iii)] is one of the main reasons for the interest in that frequency band. On the other hand, the need for small-sized antennas [item ii)] and high channel reuse [item i)] also lead to the choice of the 60-GHz band.

C. LMDS's

The use of the MMW band has recently been investigated also for the distribution of broad-band services to fixed users, such as in urban or suburban environments. In fact, interactive video services (IVS's) and video on demand (VoD) are expected to become some of the most successful services in the emerging broad-band network [52]. Last-mile broad-band distribution of these services in urban environments can be achieved by means of several media. One of these is wireless communication. The ease and speed of deployment are the main advantages of the wireless system with respect to the wired one. In fact, at the beginning of service deployment, competition among different network providers will benefit from the possibility of a flexible connection to the network for individual users. In this perspective, the LMDS based on wireless links at MMW is usually considered [53].

Let us focus our attention on VoD: Fig. 3 shows the architecture of the network connecting the video server to the subscriber's set-top box on a demand basis. The set-top box includes the decoding and interactivity functions and the network interface. The broad-band network creates the connection between the video server and the base stations in the LMDS system. The latter provides the last-mile access to the user; it consists of a set of overlapping microcells with base station transceivers mounted on suitable sites. Each base station provides a given number of channels, which depend on several parameters related to population density, service penetration, cell size, etc. Each channel carries the information related to an individual subscriber, consisting of a video stream having a bit rate, after Moving Picture Experts Group (MPEG) encoding, in the range from 1.5–15 Mbit/s, but typically less than 6 Mbit/s. Since the distribution of interactive systems involves a cellular structure (with multiple point-to-point connections) instead of one point-to-multipoint link, it requires an overall data rate on the order of several tens of megabits per second (depending on the multiplexing techniques adopted).

In the United States, frequencies between 27.5 and 28.35 GHz and between 29.1 and 29.25 GHz have been recently allocated for LMDS, with the aim of avoiding congestion and providing new services, particularly in urban environments [8]. In Europe, suitable bandwidth allocation is under investigation: some proposals consider frequencies between 40.5 and 42.5 GHz [10], [11]. The main reason for the choice of these frequencies is the large spectrum availability [item iii)].

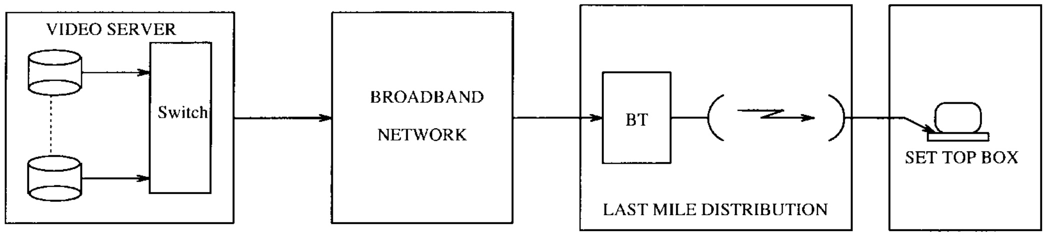

Fig. 3. VoD service components.

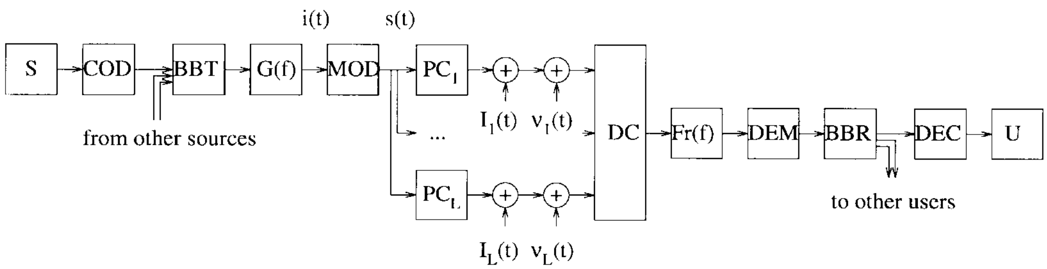

Fig. 4. Transmission system.

III. The Short-Range Transmission System

The block diagram of the transmission system under a unified design approach is shown in Fig. 4. It takes the effects of the actual propagation channel into account, including multipath propagation and the presence of interfering signals, as well as thermal noise. It also includes forward error correction (FEC) and some form of antenna diversity to counteract propagation channel impairments. The complexity of the different forms of implementation depends on the specific application.

As shown in Fig. 4, the digital source S feeds the transmission system with a bitstream having bit rate B_r. This stream may be considered either a continuous or a packetized flow; this depends on the service and the application considered. The input bitstream is first encoded by the channel encoder (COD), which includes the possible interleaving processing. Its output feeds a baseband processing block (BBT), which includes multiplexing functions, for point to multipoint links and baseband processing for modulation and multicarrier transmission. In point-to-multipoint applications, the transmission system provides a capacity, in terms of bit rate, of $B_{rt} = B_r U_G$, where U_G is the number of users the system is able to serve. At the output of BBT, the sequence of complex samples is utilized to obtain a spectrally shaped baseband complex signal $i(t)$ by using signal pulses having Fourier transform $G(f)$. The modulator MOD produces the modulated signal, $s(t)$, used for transmission, whose spectrum is centered at frequency f_o.

Due to the implementation of L antennas or an L-sector antenna at the receiver, L copies of the transmitted signal reach the receiver through L different propagation channels, $PC_i, i = 1, \cdots, L$. The ith generic propagation channel is described in the next subsection. The useful signal is impaired at each diversity branch by additive white Gaussian noise (AWGN) $\nu_i(t)$ and additive cochannel interference $I_i(t), i = 1, \cdots, L$. These undesired terms are assumed to be statistically independent. The diversity combiner (DC) is considered in this paper as a selection combiner. The signal at the output of the combiner is processed by the receiver filter, having transfer function $F_r(f)$, and then demodulated (DEM). The baseband processing block at the receiver (BBR) tries to regenerate the transmitted bitstream, which is then decoded by the channel decoder (DEC) and delivered to the user (U).

To be more detailed in the transmission system description, in the following, we will distinguish between two situations.

1) Wide-band systems (that is, systems that require, due to high data rates, a wide-band model for channel propagation). When frequency selectivity effects are present, suitable countermeasure techniques have to be introduced. In the following, OFDM with coding is considered [54].
2) Narrow-band systems (that is, systems that do not require a wide-band channel model due to low data rates with respect to medium delays). The use of antenna diversity, in conjunction with error correction and interleaving, is considered for performance improvement [55], [56].

To counteract the frequency selectivity and to exploit, by means of coding, the inherent diversity of a wide-band channel, the OFDM transmission technique is adopted [54]. Multicarrier techniques and OFDM were proposed several years ago [57]–[60], but practical implementations have only recently come about [61], [62]. With respect to adaptive equalization, time-expensive trainings are avoided, but an increased sensitivity to nonlinearities and carrier recovery inaccuracies requires appropriate consideration [63]–[65].

The frequency selectivity introduced by the multipath channel is counteracted in OFDM systems by splitting the digital information to be transmitted over N narrow-band carriers, equally spaced by Δf, in a bandwidth B_c. In this way, each narrow-band carrier, if the number of carriers is suitably selected, is subjected to flat fading conditions. If Δf is taken to be equal to the reciprocal of the useful symbol period T_s, the modulated carriers form an orthogonal set and the information can be recovered even though signal spectra overlap in the frequency domain. The modulation and demodulation processes can be efficiently implemented by means of an inverse fast Fourier transform (FFT) and FFT procedure, respectively. This implementation is known in the literature as the discrete multitone technique (DMT) [57]–[60].

In a multicarrier system, each of the N carriers is affected by different fading channels, with different received power levels, due to the frequency selectivity of the radio channel. A method to exploit the inherent frequency diversity is to use coded transmission. Hence, in this paper, linear block coding is considered with special attention to Reed–Solomon coding with and without erasures correction [66]. Another method can be devised in a point-to-multipoint system, e.g., in the downlink of a cellular system: it is possible to suitably select the subset of N_u carriers to be assigned to each user, in an adaptive way [67], with the aim of providing the best carrier set to each user, i.e., the N_u carriers with the lowest attenuation values (for that user). This method also allows each user to utilize the available frequency diversity by choosing, in the absence of contention, the best N_u of N available carriers.

When the required bandwidth is small enough to avoid frequency selectivity effects, a traditional single-carrier system is better suited. In this case, multipath fading should be counteracted by means of antenna diversity. FEC becomes effective when the use of a practical interleaving allows the exploitation of time or frequency (e.g., in conjunction with frequency hopping) diversity. The single-carrier system can be interpreted as the case with $N = 1$.

As far as the modulation format is concerned, different choices are possible as a tradeoff between performance and implementation complexity. In this paper, the different systems are investigated by considering the use of binary phase shift keying (BPSK), quartenary (Q)PSK, and quadrature amplitude modulation (QAM) with coherent detection and minimum shift keying (MSK) with noncoherent detection. Proper evaluation of their performance requires accurate choice of the propagation channel model, which is provided in the next subsection.

A. The Propagation Channel

In indoor environments, the electromagnetic field at MMW tends to be confined by walls due to their electromagnetic properties at these frequencies. In outdoor environments, at frequencies around 60 GHz, an additional attenuation due to oxygen absorption limits the transmission range.

In the applications considered, due to multiple reflections and diffraction effects, the signal arrives at the receiver through different paths. Their superposition causes multipath fading at the specific location and frequency selectivity in wide-band systems. The wireless propagation channel can be modeled as being time invariant or very slowly time variant by means of the low-pass transfer function

$$H_0(f) = \sum_{l=1}^{Z} a_l e^{j\theta_l} e^{-j2\pi f \tau_l} \tag{1}$$

where Z is the number of rays and a_l, θ_l, and τ_l are the amplitude, phase, and delay of the lth ray, respectively [55]. In our analytical framework, the definition of $H_0(f)$ does not include antenna gains; it only includes the propagation medium and the normalized radiation pattern of the antennas (normalized channel).

The assumption of a time-invariant characterization is reasonable when:

- the receiver position is quasistationary and the effects of moving objects are negligible; this is true for indoor LAN's and also tends to be true in outdoor LMDS's when suitable position and orientation are chosen for the antenna;
- in packet data transmission the data rate is sufficiently large with respect to channel variations; this tends to be true in those ITS applications where the Doppler bandwidth (proportional to v/λ, where v and λ denote the speed of user and the wavelength, respectively) remains much smaller than the data rate.

At MMW, even in the case of short-range links, it is particularly useful to characterize separately the *small-scale* (in a range of about 20 wavelengths) and *large-scale* behavior of the propagation channel.

For indoor LAN and outdoor LMDS applications, in the small-scale rays, amplitudes and delays do not significantly change when moving the receiver, whereas phases are characterized by large variations. Therefore, amplitudes, delays, and Z are usually fixed in the small scale according to measurements or ray tracing evaluation, whereas phases θ_l $(l = 1, \cdots, Z)$ are assumed to be independent random variables uniformly distributed in the range $[0, 2\pi]$. For ITS applications, this is considered to be true in the horizontal plane, when the transmitter is stationary. Indeed, in the vertical plane in line-of-sight conditions, there is often a road-reflected ray that is strongly correlated with the direct one, and a dominant deterministic component originates from their superposition. In intervehicle communications, where both the transmitter and the receiver move, even when their distance is fixed, amplitudes, delays, and Z in the horizontal plane change in the small scale due to the movement of the surrounding context.

In those applications where the bandwidth is sufficiently narrow to avoid frequency-selective effects, the knowledge of $H_0(0) = \Gamma e^{j\phi}$ is sufficient to characterize propagation channel effects; Γ and ϕ denote the gain and phase introduced by the normalized channel, respectively. In this case, a statistical model is usually introduced. The most common models for envelope Γ are the Rayleigh and Rice models; the latter is adopted especially when a dominant fixed component (LOS) characterizes small-scale propagation [55], [56].

The large-scale variations of the propagation channel can be evaluated in a grid of receiver locations spaced by at least some tenth of wavelength.

To synthetically characterize the channel, we refer to path loss PL and delay spread $\tau_{\rm rms}$ as

$$PL = \frac{1}{\sum_{l=1}^{Z} a_l^2} \tag{2}$$

$$\tau_{\rm rms} = \sqrt{\overline{\tau^2} - \overline{\tau}^2} \tag{3}$$

where

$$\overline{\tau} = \frac{\sum_l a_l^2 \tau_l}{\sum_l a_l^2}, \quad \overline{\tau^2} = \frac{\sum_l a_l^2 \tau_l^2}{\sum_l a_l^2}. \tag{4}$$

Another significant parameter used to describe channel effects, in the small scale, is the K factor, defined as

$$K = \frac{a_{\max}^2}{1/PL - a_{\max}^2} \tag{5}$$

where $a_{\max}$ is the amplitude of the strongest ray. It becomes the Rice factor when a Rice statistical model is adopted to characterize narrow-band propagation [55], [56].

With the purpose of thoroughly investigating channel propagation by avoiding expensive measurements, deterministic methods are suggested for the analysis of microcellular systems at MMW [55], [68]. More particularly, in recent years, new methods have been developed that involve the use of site-specific propagation models and graphical information system data bases. One of these methods is based on ray tracing techniques [23], [69].

IV. The Framework for Performance Characterization

The aim of this section is to define a common framework for performance assessment of the different applications considered. We distinguish between link and protocol performance figures: in the former case, bit and packet error probability are considered, whereas in the latter, we introduce some metrics related to the delay in packet delivery, which is of interest for real-time services, such as in the case of video, voice, or ITS applications (emergency warning, etc.).

With the view of considering, as a first step, link performance figures, we emphasize the idea of defining service- and user-oriented metrics. In fact, the choice of the metric that is best suited for performance evaluation depends on the kind of service, since different applications are sensitive to the time structure of error patterns in data reception in different ways. To be more precise, let us define a parameter t_W as the time window that reflects the ability of the user to distinguish an error pattern. As an example, video transmission (as in LMDS applications) is characterized by large values of t_W (on the order of 100–300 ms), since the user sensitivity can seldom distinguish channel conditions giving bad video quality for time intervals shorter than 100–300 ms. We can call this phenomenon an *averaging user process*. A similar effect is found in voice applications with proper values of t_W. On the other hand, when the user is a machine, like a personal computer in a WLAN or the on-board computer unit of a vehicle equipped with an IVC or RVC system, the time window t_W is much shorter, on the order of a packet time (that is, milliseconds or less).

To make the right choice of performance metrics, the value of t_W, typical of the application, has to be compared with the coherence time t_C of the small-scale variations [55]: when t_W is larger than t_C, it can be assumed that the averaging user process leads to an *average* perceived quality, whereas if t_W is shorter than t_C, the quality is a function of channel small-scale fluctuations. In the former case, an averaged (over small-scale channel variations) performance figure has to be chosen; in the latter, a metric related to the cumulative distribution of channel variables has to be used. It is worth noting that even though this holds either for the MMW band or at lower frequencies, it assumes a major relevance when the wavelength is very short, since the rate of small-scale variations can be high even for quasistationary users.

Keeping this concept in mind, and with the aim of introducing the definition of small- and large-scale performance figures, let us first define the link performance metrics, that is, the error probabilities at the output of the transmission system for a given user when transmitter and receiver positions are fixed and the propagation channel is stationary. As performance measures, we use the bit error probability P_b and the packet error probability P_p. In case of linear block coding, code-word error probability can be considered as well. In the general case of multicarrier transmission, when neglecting interfering signals, these figures can be obtained as functions of the vector of the samples of $H_0(f)$ [70], i.e., $|H_n|^2 = |H_0(n \cdot \Delta f)|^2, n = 0, \cdots, N-1$ and the parameter normalized signal-to-noise ratio (NSNR) as follows:

$$P_b = F_b\left(|H_0|^2, \cdots, |H_{N-1}|^2, \text{NSNR}\right) \tag{6}$$

$$P_p = F_p\left(|H_0|^2, \cdots, |H_{N-1}|^2, \text{NSNR}\right). \tag{7}$$

The parameter NSNR has been defined as

$$\text{NSNR} \cdot |H_n|^2 = \frac{E_{bn}}{N_o} \tag{8}$$

where E_{bn}/N_o is the SNR at the receiver, evaluated over a bandwidth equal to B_{rt}, for the nth carrier; hence

$$\text{NSNR} = \frac{P_t G_t G_r}{k T^o B_{rt}} \tag{9}$$

where P_t is the average transmitted power, G_t is the transmitting antenna gain, G_r/T^o is the receiver sensitivity, and k is the Boltzman's constant.

When performance is evaluated in the presence of interference, the previously defined error probabilities also depend on the vectors of interfering channels' frequency response samples, introducing a set of potentially very large parameters. Having in mind the applications to be investigated in this work, it is more interesting to specify this function for single-carrier transmission $(N = 1)$ and narrow-band channel modeling. This topic has been thoroughly investigated in [29]–[31], where the following simplified evaluation has been proposed:

$$P_b = F_b^{(I)}(U, U/I, N_I) \quad (10)$$

$$P_p = F_p^{(I)}(U, U/I, N_I) \quad (11)$$

where N_I represents the number of interfering signals, U is the useful SNR at the receiver given by

$$U = \text{NSNR} \cdot \Gamma^2 \quad (12)$$

and U/I is the carrier-to-interference ratio.

It is emphasized in [29] that for N_I ranging from zero to two or three, the performance can be very sensitive to the value of N_I. The role played by N_I is also discussed in [32].

The general approach introduced by (10) and (11) allows proper consideration of the capture effect in packet communication as a function of N_I.

In the following subsections, the definition of the performance figures suitable to characterize MMW communications is given.

A. Local Performance

By utilizing the performance analysis in static conditions, we can first characterize the small-scale system behavior, i.e., in a range of about 20 wavelengths (e.g., 10 cm at 60 GHz). It has already been mentioned that small-scale channel fluctuations depend on phase variations (in ITS applications, also on amplitude and delay variations) of the rays arriving at the receiver, thus resulting in error-probability fluctuations.

In every small-scale area, a mean (locally averaged) bit or packet error probability can be defined as a performance index useful to characterize the performance of applications concerning voice and video transmission. For high-speed data transmission between stationary or slowly moving terminals, a local outage probability better characterizes system performance because it indicates the probability of satisfying a given performance requirement when the terminal is randomly placed in the local area under consideration. More precisely, "slowly moving terminal" means a receiver that remains stationary with respect to the transmitter terminal in a packet time. Hence, we will use $\overline{P_b}$ and $\overline{P_p}$ to indicate the local mean of bit and packet error probability

$$\overline{P_b} = E[P_b] \quad (13)$$

$$\overline{P_p} = E[P_p] \quad (14)$$

whereas we will define the local outage probability as

$$\pi_b = \text{Prob}\{P_b > \sigma_b\} \quad (15)$$

$$\pi_p = \text{Prob}\{P_p > \sigma_p\} \quad (16)$$

for bit and packet, respectively. Here, σ_b and σ_p are suitable thresholds that should be set to $10^{-8 \div -10}$ and $10^{-6 \div -8}$, respectively, if we want to approach the wire transmission quality. However, values around $10^{-2 \div -4}$ may be considered when suitable automatic-request techniques [66] are implemented.

When a wide-band channel description is utilized, the evaluation of the performance metrics introduced above is usually semianalytical, as follows:

- a set of channels in a given large- or small-scale area is generated according to ray-tracing evaluation, measurements, or suitable statistical models similar to that presented in the previous section;
- then, the corresponding set of bit or packet error probabilities is analytically carried out by utilizing suitably defined algorithms (see, e.g., [7]–[9]);
- last, from this set, mean and outage are evaluated by means of Monte Carlo procedures.

On the other hand, the method for evaluating outage and mean error probabilities can be analytical when a narrow-band channel description is adopted and a suitable statistical model for local fading is considered. Several evaluation examples of the local outage probability when Rayleigh, Rice, or Nakagami small-scale fluctuations are considered can be found in [71]–[80], where useful and interfering signals are considered with a narrow-band channel model.

To be more precise, let us evaluate the local outage probability given by (16), π_p, when (11) holds. Having fixed the desired link quality in terms of packet error probability σ_p, it can be derived [30], [31], [43], [81] as

$$\pi_p = 1 - \text{Prob}\{U > \beta; U/I > \alpha(U, N_I)\} \quad (17)$$

where β is the minimum value of U required to obtain the desired link quality σ_p in the absence of interference (AWGN channel) and $\alpha(U, N_I)$ is the signal-to-interference protection ratio, related to σ_p. The signal-to-noise threshold and the protection ratio depend on the transmission system and the multiple access method considered, the countermeasures employed, and the quality desired. The combined effects of thermal noise and interference require $\alpha(U, N_I)$ to be evaluated as a function of U and N_I. A more general and complete description of the approach can be found in [30] and [31], where the impact of the number of interferers on the performance is outlined.

B. Large-Scale Performance and Coverage

Besides the local characterization, a large-scale characterization can be carried out to support coverage analysis. Large-area average error probability can be useful to characterize wireless data network performance with a given multiple access protocol, as in [81], or to characterize continuous transmission services in mobile environments, but it is not representative of coverage. A way to define coverage is to consider the probability that the transmission does not meet the quality requirements when the receiver is randomly placed in a large zone (e.g., the room) as in indoor wireless data networks [46]. This is given by the large-area outage probability, defined as

$$\Pi_b = \mathrm{Prob}^{(L)}\{P_b > \sigma_b\} \quad (18)$$
$$\Pi_p = \mathrm{Prob}^{(L)}\{P_p > \sigma_p\} \quad (19)$$

where $\mathrm{Prob}^{(L)}$ indicates a large-scale statistical evaluation. An example of derivation of the large-scale outage probability can be found for narrow-band modeling of mobile channels (i.e., Rice fading with log-normal shadowing superimposed) in [82].

It is our opinion that a more significant definition of coverage should consider the relative number of small-scale zones in a given environment where the receiver, if randomly placed, can work satisfactorily with an acceptable local mean error $\overline{P_b}$ ($\overline{P_p}$) or local outage probability π_b (π_p). An acceptable level of local outage probability may be 10^{-2} for broad-band indoor radio networks. The definition of coverage introduced above is particularly useful if we are interested in obtaining a coverage map composed of an ensemble of small-scale zones where the terminal could be placed.

Therefore, the performance in a large area can be defined by considering the coverage probability, that is, the probability that, for each link, the quality requirements in terms of link performance are fulfilled

$$P_{\mathrm{cov}} = \mathrm{Prob}\{X < Q\} \quad (20)$$

where X is the small-scale performance parameter (local mean error or local outage probability) and Q is a suitable threshold fixed as a function of the requirements. It is worth noting that the previously outlined definitions of coverage are quite general because they take the effects of multipath propagation into account, in addition to channel attenuation and interference, as well as a user-oriented quality definition.

In this case, the evaluation method of large-scale performance figures is semianalytical, which means that a set of channels in a given large-scale area is generated according to ray tracing evaluation or measurements for the given environment, and the corresponding set of local or static bit or packet error probabilities is carried out as indicated before. More precisely, the coverage is obtained from the ensemble of local performance figures.

C. Protocol Performance

The link performance metrics introduced are related to the behavior of the transmission system due to channel impairments and the amount of countermeasure techniques introduced. On the other hand, in a multiuser context, the multiple access protocol plays a relevant role since reuse strategies and channel allocation schemes have a great impact on the performance of the application considered.

Typical performance measures, for network (and protocol) assessment, are related to throughput and delay; several choices can be made since they are random variables, related to the position (large-scale) of the terminals, whose statistics can be described by means of average or cumulative values [81]. Well-known expressions of throughput hold for simple access protocols, such as, e.g., ALOHA and slotted-ALOHA [83], [84]. As far as delay is concerned, its cumulative distribution function is of great interest for real-time applications, where average values of delay do not represent a good performance measure since the application is delay sensitive in the sense that delays larger than a given threshold are to be avoided (see, e.g., [85]).

We would like to stress that, either in the case of throughput or delay, the protocol performance metric strongly depends on the link performance measure [86]. Hence, through suitable evaluation of bit or packet error probability, as a function of channel conditions, protocol performance can be assessed. To clarify the mentioned concept, let us introduce an example of a protocol performance metric that can be applied to an ITS scenario. Let us consider a network in a monodimensional scenario with N_v terminals, each of them transmitting packets in the forward direction only. Let us also investigate a multiple access scheme based on R-ALOHA, that is, a contention protocol [43], [85]. In R-ALOHA, the time resource is subdivided into frames of equal duration, each of them consisting of a number N_s of time slots. Now, let us assume that all terminals simultaneously compete for one of N_s channels starting from a memoryless state, where no information on free and collision channels is available (worst case). We define the first success time (FST) as the number of frames that elapse until a given terminal succeeds in correctly transmitting its packet, that is, until it receives the acknowledgment by the receiver. FST is not a function of N_v as long as N_v is sufficiently large. It obviously depends on the packet capture probability P_c in each link, which can be evaluated as $P_c = 1 - P_p$. On the other hand, the packet capture probability can also be analytically assessed by means of a capture model [81], [87], which leads to an expression of P_p similar to that of local outage probability π_p, that is, for a narrow-band channel model, (17)

$$P_p = 1 - \mathrm{Prob}\Big\{U > \beta^{(o)}; U/I > \alpha^{(o)}(U, N_I)\Big\} \quad (21)$$

where $\beta^{(o)}$ and $\alpha^{(o)}$ are suitably defined thresholds.

Under these considerations, the FST takes the local fluctuations of fading in a small time interval (a few frames) into account. To obtain an overall metric, which represents the behavior of the network, the deadline failure probability (DFP) can be defined as

$$\mathrm{DFP} = \mathrm{Prob}\,[\mathrm{FST} > D] \quad (22)$$

where D is the maximum delay, expressed in terms of frames or slots, required for the successful transmission of one packet. It represents a network performance metric referred to a user placed in a small-scale given position.

V. Intelligent Transport Systems

Let us consider an ITS application based on both RVC and IVC systems (as in Fig. 1). For the sake of simplicity, a single-lane road scenario is investigated, where

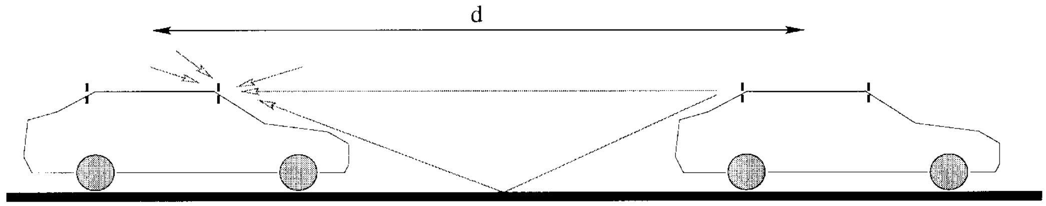

Fig. 5. Channel model for IVC in the 60–64-GHz band.

beacons are exploited to collect data from vehicles and transmit information about traffic conditions. According to a monodimensional architecture, characterized by a spacing of $2R$ meters between adjacent beacons, each beacon covers a cell of radius R. Let us assume that a channel is assigned to each vehicle and investigate the downlink case.

Beacons have omnidirectional antennas, covering their cell. Each vehicle in the network is assumed to be equipped with a communication device and four directional antennas: two of them radiate in the backward and two in the forward direction. Each couple of antennas represents a two-branch height diversity system where the two elements are vertically separated by a fixed distance [39]. Antenna heights with respect to flat terrain are assumed to fluctuate due to ground unevenness around their mean values, and fluctuations are modeled by a sinusoidal law with frequency 1 Hz. The modulation technique considered here is single-carrier MSK, allowing a noncoherent demodulation process that is obtained in this case by means of a limiter-discriminator (LD) detector.

For RVC and IVC systems in the 60–64-GHz band, channel modeling should take into account the presence of the road surface. More precisely, a model based on a direct path, a road-reflected path, and a multipath component has to be assumed when LOS conditions occur (see Fig. 5) [5], [39]: the received power at distance d derives from the coherent cumulation (that is, taking proper phase properties into account) of the road-reflected and direct components, and the incoherent sum with the Rayleigh-faded multipath power. On the other hand, in NLOS conditions, a simple Rayleigh-fading model can be assumed.

A group of N_v mobiles separated by an intervehicle distance d_{iv} is considered. Vehicles can communicate with beacons (RVC) and among them (IVC system). In both cases, they transmit packets of 250 bits.

As a particular example, for the RVC system, we refer to a frequency/time-division multiple access scheme, where the total number of channels (slots) is split into N_q sets of U_G time-division multiplex channels. Each set of channels is assigned to a cell and spatially reused. A group of N_q cells, using all the channels, represents the cluster, and N_q is the cluster size.

For the IVC system, a multiple access scheme similar to that described as an example in the previous section, based on R-ALOHA, is considered. Moreover, a time division duplexing scheme is implemented. The frame structure is subdivided in two parts. In the first part, N_s slots are used for backward transmission (hence, transmitters are linked to backward and receivers to forward antennas); in the second part, acks are sent in the forward direction. A multihop strategy is introduced, which requires only direct transmission to the preceding and following vehicles; hence, only one vehicle at a time is the destination of a packet. The transmission of acks is also used for sending data in the forward direction.

The bit rate B_r, for both the IVC and the RVC systems, is on the order of a few megabits per second [4], [42], [43]. In this paper, we assume $B_r = 2$ and 1.25 Mbit/s for RVC and IVC, respectively. This allows a narrow-band modeling of channel propagation. Hence, a general description of the packet error probability can be given through (11), where the maximum number of interferers N_I is equal to two or one in the RVC and IVC cases, respectively.

A. Performance Metrics and Evaluation

As a performance measure, we consider the local outage probability (16), since the application is sensitive to the loss of single packets [35], [42]. Hence, (17) is used. For the MSK modulation scheme with LD detection and by fixing σ_b equal to 10^{-5}, leading to satisfactory values of error probability in the presence of suitable error-correcting coding schemes, the value of β is fixed to 12.5 dB. Moreover, function $\alpha(U, N_I)$ is given in [42] for $N_I = 2$. As far as the statistical model of U and I is concerned, the reader can refer to [42] and [43], where the two-ray Rice model is described.

Let us first consider the RVC system: to emphasize the advantage of the MMW band, we compare the performance of the above-described system at 60 and 5.8 GHz (the two bands are considered for these applications [33]). In Fig. 6, the local outage probability is shown as a function of R and by considering the vehicle's being on the cell edge (link distance equal to R); the same channel model is assumed for the two cases, and the same set of system parameters (transmitted power, antenna gain, etc.) is chosen (see details in [42]). The main difference between the two systems is due to oxygen absorption, which introduces a specific attenuation of 15 dB/Km at 60 GHz (whereas it is absent at 5.8 GHz). The cluster size is $N_q = 3$.

The figure shows that for short-range applications, there is no optimum value of R at 5.8 GHz due to the absence of oxygen absorption; on the contrary, at 60 GHz, a lower value of outage probability is found if the optimum value of R is chosen. Since from the spectral efficiency point of view microcellular structures perform better than macrocellular structures, it can be concluded that at 60 GHz, better performance can be achieved when fixed spectral constraints

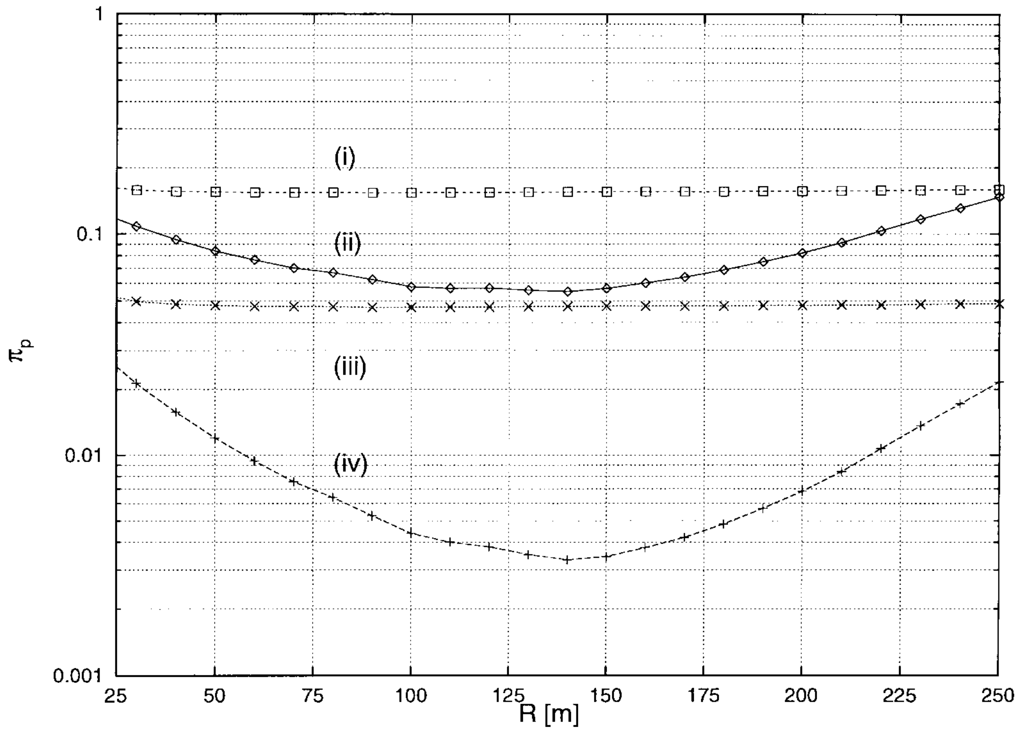

Fig. 6. Local outage probability referred to $\sigma_b = 10^{-5}$ (MSK, LD detection) against cell radius $R; N_q = 3$. Useful terminal at cell border. Comparison between 60 and 5.8 GHz; without diversity [(i): 5.8 GHz; (ii): 60 GHz] and with diversity [(iii): 5.8 GHz; (iv): 60 GHz].

are given. It is worth noting that similar results can be obtained whatever the value of the carrier frequency in the 60–64-GHz band since in that range, oxygen absorption is significant.

Now, let us consider the IVC system and evaluate the DFP defined in the previous section. As far as the packet capture model is concerned, for the sake of simplicity, we in this case neglect the dependence of $\alpha^{(o)}(U, N_I)$ from U and assume, as an example, $\alpha^{(o)} = 2.5$ dB, which holds for U tending to infinity and $N_I = 1$ [43]. Moreover, $\beta^{(o)}$ is fixed to 9.8 dB.

In Fig. 7, DFP is described in terms of the number of slots instead of the number of frames. The figure shows the results of a simulation carried out in accordance with the previously defined scenario: DFP increases when increasing N_s. Hence, small values of N_s have to be chosen, and the results of Fig. 7 suggest the choice $N_s = 5$.

The results shown in this section emphasize the role played by oxygen absorption on interference control methods and cell planning, as announced in the introduction. Indeed, unlike traditional cellular systems working at microwaves, an optimum value of cell size can be found. This effect could be further investigated by considering, as an example, bidimensional cellular environments.

VI. High-Speed Indoor Wireless LAN

This section investigates a high-bit-rate (100–155 Mbit/s) coded OFDM system for high-speed indoor wireless networks at 60 GHz [7], [70]. The role of coding, frequency diversity, and antenna directivity/sectorization is investigated and underlined. The sector selection strategy adopted is based on the measure of the power received from each sector in the frequency band of the system. Sectored antennas allow an additional directivity and diversity gain as well as an improved flexibility for the user in antenna placing because orientation problems are avoided.

As far as propagation in actual environments is concerned, the Telecommunication Laboratory of our department in the Centro di Studio per l'Informatica e i Sistemi di Telecomunicazioni (CSITE) building has been considered. It is 3 m high, and its layout is described in Fig. 8. It contains the following materials: 10-, 6-, and 3-cm-thick plasterboard walls, wood (doors and furniture), glass (windows), metal (doors and other). The furniture consists of six racks having a dimension of $3 \times 1 \times 2$ m^3 and characterized by 2-cm-thick wood.

For this scenario, small- and large-scale channel characterizations were obtained by means of ray-tracing modeling in [22] and [23]. Channel characterization was developed by fixing the transmitter in the middle of the room at ceiling height (see Fig. 8) and by considering, as a reference, omnidirectional antennas in the horizontal plane with vertical polarization to cover the whole room.

Large-scale variations were tested by moving the receiver on a grid of 1700 points with about 0.25-m step. A "room partitioning" description was introduced in [23]: it considers the propagation environment to be partitioned in several zones, including points (where the receiver can be placed) lightened by the same set of reflectors and having a common large-scale description. There is a LOS, as well as several

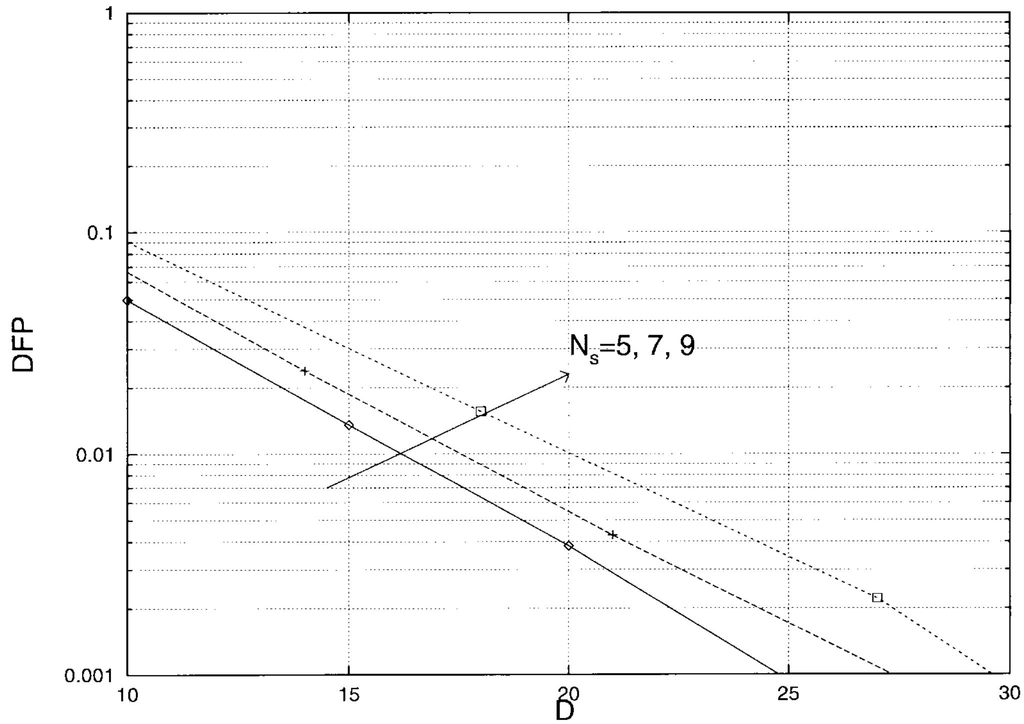

Fig. 7. DFP as a function of the number of slots D; $N_v = 31, d_{iv} = 20$ m; 100 000 iterations.

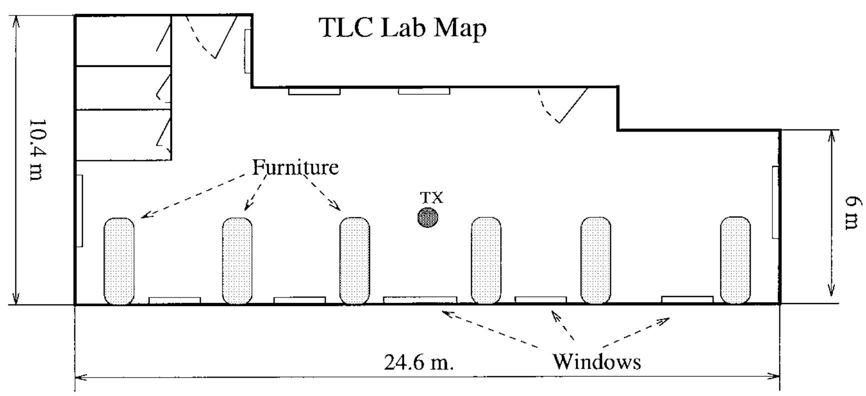

Fig. 8. The Telecommunications Laboratory (TLC) of our department in the CSITE building.

NLOS zones. In NLOS zones, the large-scale received power is much smaller with respect to the LOS zone (at least 10–20 dB). The indoor radio system experiences a path loss ranging from 60 to more than 120 dB and a $\tau_{\rm rms}$ up to 20 ns with factor K varying from -5 dB to several tenths of decibels.

An ideal sectored radiation pattern is considered for the receiving antenna. It should be noted that the reference orientation angle of sectors is considered as a uniformly distributed random variable in the range $[0, 2\pi]$. By comparing four sectors and six sectors receiving antennas with the omnidirectional one, whatever the system configuration, it has been found that the amount of NLOS points with $\tau_{\rm rms} > 10$ ns is reduced from 20% to 6–8% while parameter K increases. The joint effects of directivity gain and reduction of frequency diversity on the system under investigation will be checked later in the results.

The multicarrier technique adopted for this application is the coded OFDM, described in the appendix. For the sake of clarity, the meaning of some symbols used in the appendix is reported: N_a represents the number of available channels, M the number of modulation states, T_g the guard time, R_c the code rate, and ξ_D the spectrum efficiency reduction factor. According to that description, the following assumptions have been made: $N_a = N_u, M = 4$ with $A_n^k \in \{+1, -1, +j, -j\}, T_g = 50$ ns. The use of clustering is a viable way to reduce FFT complexity and sensitivity to system nonlinearities: clustered systems have been investigated in [7].

A. Performance Metrics and Evaluation

Performance analysis can be carried out by means of analytical algorithms developed to obtain the error probabilities, as defined in (6) and (7), for the coded OFDM

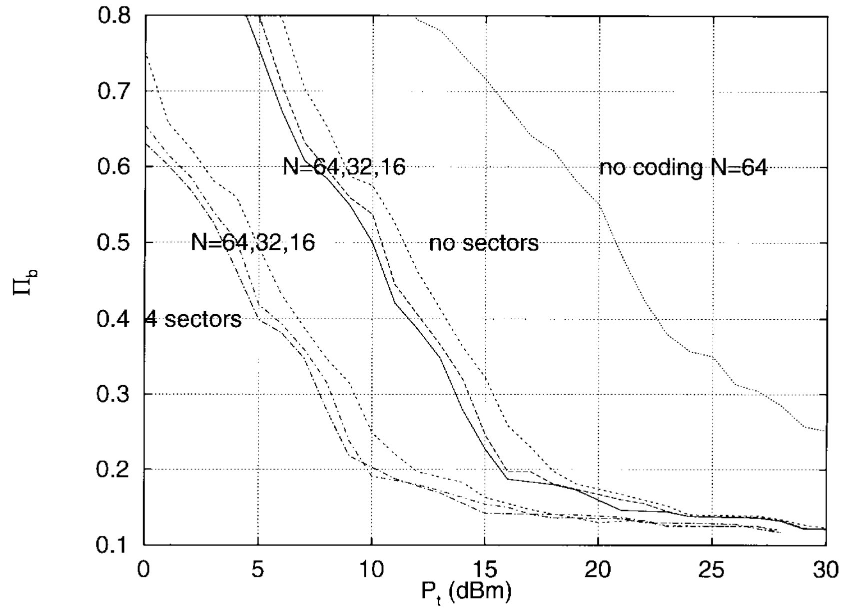

Fig. 9. Large-area outage probability in the NLOS zones with different number of subcarriers with and without sectorization.

system when transmitter and receiver positions are fixed and the propagation channel is stationary.

Let us start with the bit error probability at the output of each OFDM channel before decoding. The bit error probability, for the generic user, referred to the nth carrier can be easily found to be given by

$$p_n \cong \frac{1}{\log_2 \sqrt{M}} \frac{\sqrt{M}-1}{\sqrt{M}} \cdot \text{erfc} \sqrt{|H_n|^2 \text{NSNR} \frac{3 \log_2 \sqrt{M}}{M-1} \xi_D R_c} \quad n = 0, \cdots, N-1 \tag{23}$$

where NSNR has been defined in Section IV and the other parameters are defined in the appendix. Each OFDM subchannel, with respect to the coded bits, can be viewed as a binary symmetric channel characterized by the error probability p_n depending on the channel response at the frequency f_n. The performance of the block-coded OFDM system can be described by means of the postdecoding error probabilities, which are functions of the vector of the N bit error probabilities $(p_0, p_1, \cdots, p_{N-1}) = \boldsymbol{p}$ as follows:

$$P_b = f_b(\boldsymbol{p}) \tag{24}$$

$$P_p = f_p(\boldsymbol{p}). \tag{25}$$

These functions can be analytically evaluated [7], [70] for the different system configurations (i.e., use of clustering, error and erasure correction, adaptive carrier allocation [67]).

By utilizing the performance analysis in static conditions, we can first characterize the small-scale system behavior—i.e., in a range of 20 wavelengths (10 cm)—by means of local outage probabilities π_b and π_p. Large-scale characterization is usually done by means of large-scale outage probabilities Π_b and Π_p, and coverage probability referred to local outage. It has been verified that the LOS points of the room can be easily covered, whereas the most critical points are those in NLOS conditions due to high path loss and channel dispersion. For this reason, in our study, the results will mainly refer to the NLOS conditions.

In Fig. 9, we consider a system with a total antenna gain $G_t G_r$ equal to 20 dB (26 dB with four-sector receiving antenna), a receiver noise figure $F = 10$ dB, and a bit rate equal to 100 Mbit/s. It shows large-area outage probability (Π_b) referred to $\sigma_b = 10^{-9}$ and to NLOS zones of the grid plotted against transmitter power P_t. In practical applications of indoor communication at 60 GHz, maximum values of P_t on the order of 10 dBm are to be considered. In this context, Fig. 9 shows outage probability with different system configurations: an OFDM scheme is considered with and without coding and by varying the number of sectors (one and four). If we assume $P_t = 10$ dBm as a reference case, a system without sectorization shows a level of outage probability equal to about 50–60%; it decreases to about 20% by using a four-sector receiving antenna. This means that the coding gain can counteract the degradation caused by channel selectivity, but it may be not sufficient to compensate for the large path loss.

It should also be noted that the uncoded OFDM system is not able to work in the NLOS zones (large-area outage exceeding 90%). Moreover, it appears that 10% of outage probability in NLOS conditions is practically unreachable due to the very large path loss characterizing the most hidden zones. Other results can be found in [7] and [70].

For a deeper discussion of the coverage probability found in the scenario considered, [7] shows the coverage map of the Telecommunications Laboratory by considering the OFDM system, dealing with ATM packets at $B_r = 155$

Mbit/s, with or without sectored antennas and with or without coding.

VII. Local Multipoint Distribution Systems for Interactive Video Services

As far as LMDS for VoD applications is concerned, a wireless solution at 30 GHz is investigated [9]. The system is designed to deliver the VoD service in urban areas where several users share one building but use their own individual antenna to be placed on the user windows. The use of individual antennas allows individual users to buy and install an antenna and receiver by themselves. We analyze an urban cellular radio system with microcells having a radius of about 300 m. In this perspective, a multiple access technique and a new scheme for resource allocation are discussed [67].

A block of the city of Bologna in the neighborhood of the engineering faculty of the university has been considered as the application scenario, and the propagation channel has been modeled through the use of a ray-tracing software [9]. The LOS between the transmitter and the receiver could be absent, and buildings cause severe path loss. To investigate the large-scale variations of the propagation channel, we have considered a grid of 500 receiver locations spaced by at least 10 meters; antenna heights take values of 3, 6, and 9 m. The transmitting antenna is a sectorial antenna composed of four idealized sectors placed at a suitable site whose height is 30 m. An ideal antenna with uniform radiation pattern and azimuthal beamwidth equal to 40° in the horizontal plane is considered at the receiver; its orientation is chosen in accordance with the maximum received power.

Each point in the grid can be represented in the $\tau_{\rm rms}-PL$ and $K-PL$ planes, as in Fig. 10. It is worth noting a certain amount of correlation between the values of PL and $\tau_{\rm rms}$; in fact, points with large path loss also show large delay spread. On the other hand, no relevant correlation is found between K and PL, except for small values of PL (LOS conditions). From Fig. 10, we can note that the delay spread can reach a few hundreds of nanoseconds. Therefore, from the previous consideration, it appears that a service requiring several megahertz for transmission can be impaired by frequency selectivity effects.

The system investigated uses a coded OFDM transmission system (see the appendix) with an FDM multiplexing technique [9]. This system is able to supply up to U_G different channels with FDM multiplexing; each channel carries the information related to a given user and is defined by a subset of the N_a available carriers. Each channel needs $N_u = N_a/U_G$ carriers. At the receiver side, each user will select its own carrier set. As far as carrier assignment for FDM is concerned, two classes of schemes are defined and investigated [67]. In the largest distance technique (LDT), the coded message for each user is transmitted using carriers having a frequency distance as large as possible in the given allocated bandwidth, whereas in the adaptive technique (AT), the coded message is transmitted using carriers chosen by exploiting the *channel state information* (CSI). In this system, the CSI is the set of channel gains for each carrier and for each user. CSI is assumed to be known at the transmitter: this assumption seems reasonable since the IVS system provides a reverse channel [52], whose aim is the transmission of the user choices concerning the desired television channel; hence, this resource can be exploited by each user to send the part of channel information related to its channel.

This allows the system to select the proper set of carriers to be assigned to each user in an adaptive way. The purpose of this assignment is to provide the best subset of N_u carriers to each user. In [67], three different AT algorithms to face the concurrence problem were proposed and evaluated: among these, we will consider the cyclic priority algorithm, which offers the best set of carriers to the user having the highest priority; the priority is cyclically reassigned.

A. Performance Metrics and Evaluation

To evaluate the bit error probability for coded OFDM systems when the propagation channel is stationary, we refer to the algorithms developed in Section VI-B. The bit error probability of (23) is now referred to the nth carrier of the generic user; each user is influenced by a different vector of channel samples H_n. For this system, we consider values of M up to 64 and error correcting only decoding.

The equations of Section VI-B allow analytical evaluation of the user performance in a given propagation channel and carrier allocation conditions. User local performance can be evaluated by considering an average bit error probability as follows. As random phase variations could arise when small-scale variations in the receiving antenna position are considered, leading to correspondent variations even in the carrier allocation, bit error probability can be evaluated by averaging over phase changes, i.e.,

$$\overline{P_b} = E_\Theta[P_b(\boldsymbol{\Theta})] \tag{26}$$

where the dependence of P_b on phase vector $\boldsymbol{\Theta}$, which includes all the ray phases for every user, has been explicited. The ray phases appear in (23) through (26) and $|H_n|^2$. The average in (26) is computed by means of a semianalytical evaluation method involving, for a given set of fixed users, a random generation of the phases for each user propagation channel.

The performance in a large area can be defined by considering the coverage probability (20). It can be evaluated by counting the cases where the quality requirements are fulfilled when varying all the possible user positions considered (500, as mentioned before) and the set of users accessing the service; a total of 100 000 events have been taken into account. In the numerical results, the threshold $Q = 10^{-5}$ has been fixed.

As we have fixed the guard time T_g equal to 0.5 μs, the number of carriers has to be greater than 100 [9]. Rolloff factor α is fixed to 0.2, and, as a reference, a value $U_G = 24$ has been fixed.

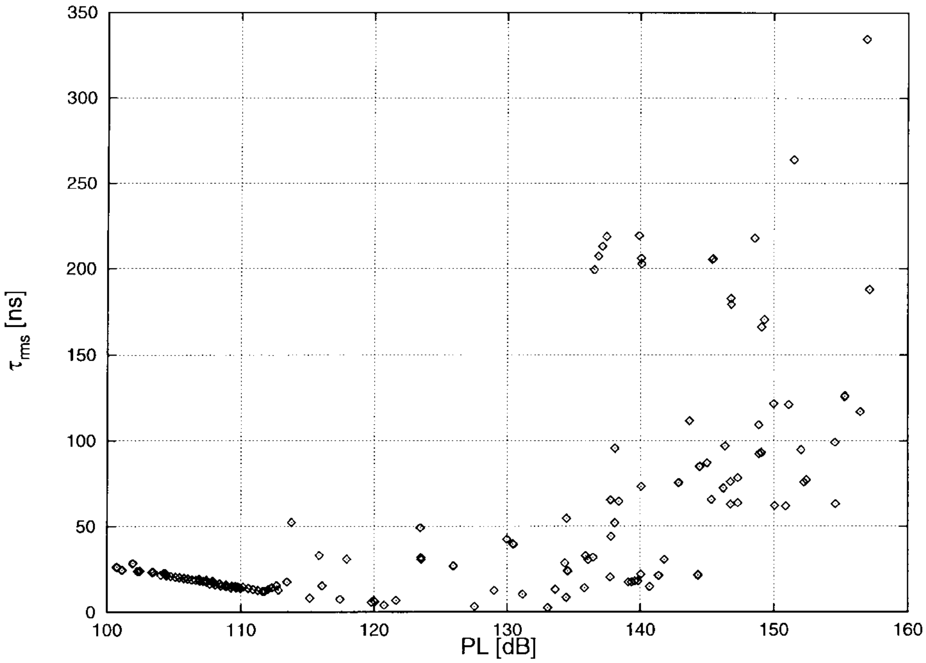

(a)

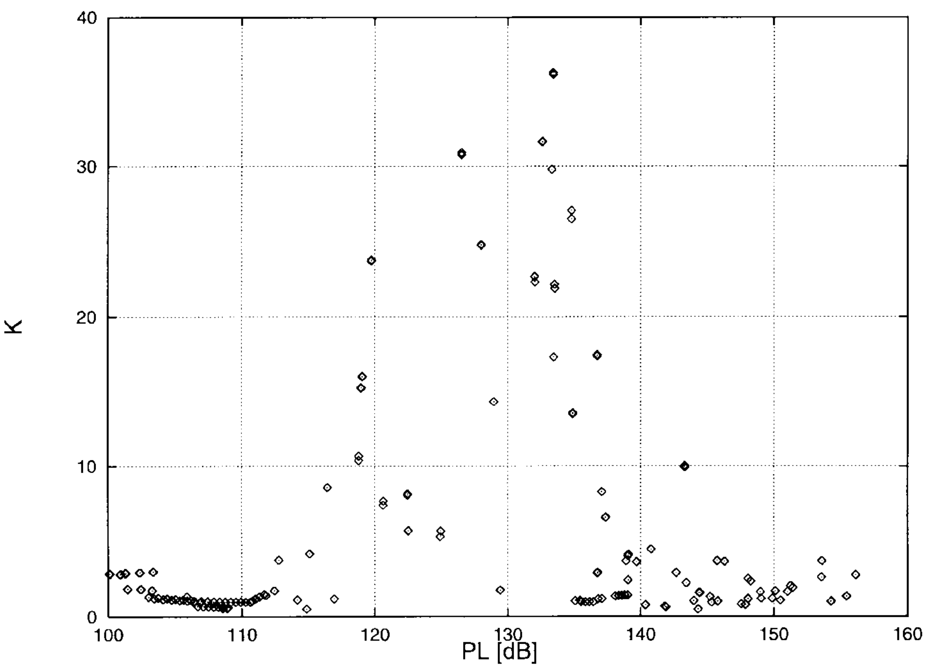

(b)

Fig. 10. Distribution of points in the (a) $\tau_{\rm rms} - PL$ plane and (b) $K - PL$ plane.

Now we analyze the coverage offered by different coded OFDM systems as a function of NSNR in the considered realistic scenario. More precisely, we study the influence of the access technique, i.e., AT versus LDT, and the sensitivity of the performance on N_t, M, and R_c, having fixed the RF system bandwidth and the code length. In Fig. 11, the bandwidth per user (B_u) and the carrier number (N_t) have been fixed to 4.3 MHz and 128, respectively, and the coverage achievable using different code rates (R_c) for a Reed–Solomon code with length fixed to 63 has been investigated. The curves show significant performance improvement due to AT technique with respect to the LDT case. In fact, a larger coverage probability can be achieved, and the improvement is on the order of 4–6 dB in terms of SNR, at a given fixed coverage probability. We can also note that in the LDT case, the best performance is obtained with a certain expense in modulation and coding complexity, e.g., by using $R_c = 1/2$. In the AT case, the achievable coding gain is limited; hence, less coding and modulation complexity is required (the best solution is between the cases $R_c = 1$ and $R_c = 1/2$). AT always yields better utilization of diversity by offering to the user the best carrier allocation.

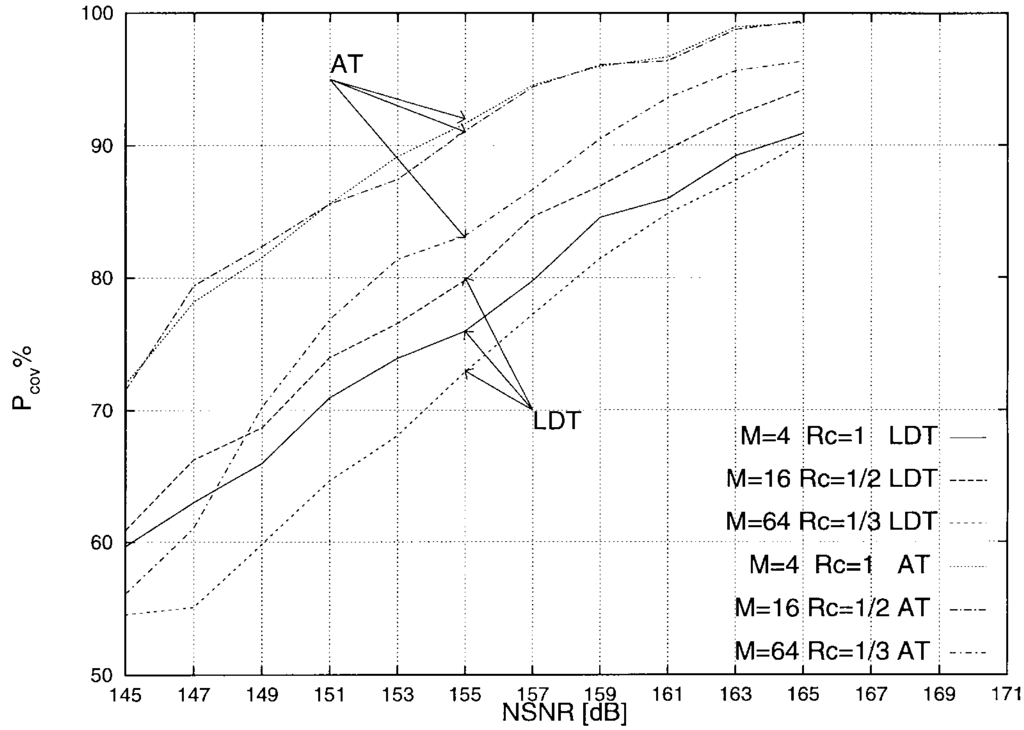

Fig. 11. Coverage probability, expressed in percentage, for coded OFDM with 128 carriers.

Table 1 Coverage Probability as a Function of Code Rate When NSNR Is Fixed to 155 dB

M	R_c	AT P_{cov}%	LDT P_{cov}%	B_u [MHz]
16	3/4	≈ 91.8	≈ 79.0	2.6
16	2/3	≈ 92.1	≈ 79.0	2.9
16	1/2	≈ 91.1	≈ 80.0	4.3
16	2/5	≈ 90.0	≈ 80.0	6.1

Last, the sensitivity of performance to the code rate is displayed in Table 1, having fixed the carrier number, the number of modulation states, and the SNR to 128, 16, and 155 dB, respectively. To obtain a good compromise between spectral efficiency and coverage probability, a system with code rate equal to 2/3 (or 3/4) is suggested in the AT case, whereas in the LDT scheme, the best results are obtained with $R_c = 1/2$.

VIII. Conclusions

Future MMW communication systems for different applications have been extensively investigated with the view of defining suitable design criteria for both narrow- and wide-band services. The use of MMW seems encouraged by the recent evolution of technology, which will permit small-size antennas and RF circuits to be designed for different wireless services. Moreover, significant advantages deriving from the use of MMW can be identified in the large spectrum availability and high spatial filtering due to oxygen absorption attenuation, thus leading to efficient spectrum usage.

Three different actual scenarios, referred to as intelligent transport system, wide-band local-area networks, and last-mile wireless interactive services, have been considered with proper evaluation of the characteristics derived by actual propagation. More precisely, a unitary framework for performance evaluation has been carried out starting from the need of defining the most appropriate quantities characterizing service quality. Both fixed and/or mobile, narrow-, and wide-band possible multimedia services have been investigated with accurate system performance evaluation.

The methodology considered allows assessment of small- and large-scale quantities and is based on both analytical and semianalytical tools for performance characterization.

Appendix
The Multicarrier Technique

The equivalent block scheme of the baseband part (including channel coding and decoding) of the system employing coded OFDM is shown in Fig. 12. The information bits d_j with bit rate B_r are first encoded with a (n_o, k_o) block code. Then, the encoded stream is serial-to-parallel converted into n_o bitstreams. In the basic scheme, these streams directly feed the N_a input channels of the OFDM modulator with $n_o = N_a$. An interface block handles other cases of interest such as $N_a = n_o/\rho$ (ρ integer when long codes are used, $1/\rho$ integer when short codes are used), or clustered systems. The figure shows a system without clustering. At the modulator V, additional inputs are forced to zero in order to insert virtual subcarriers so

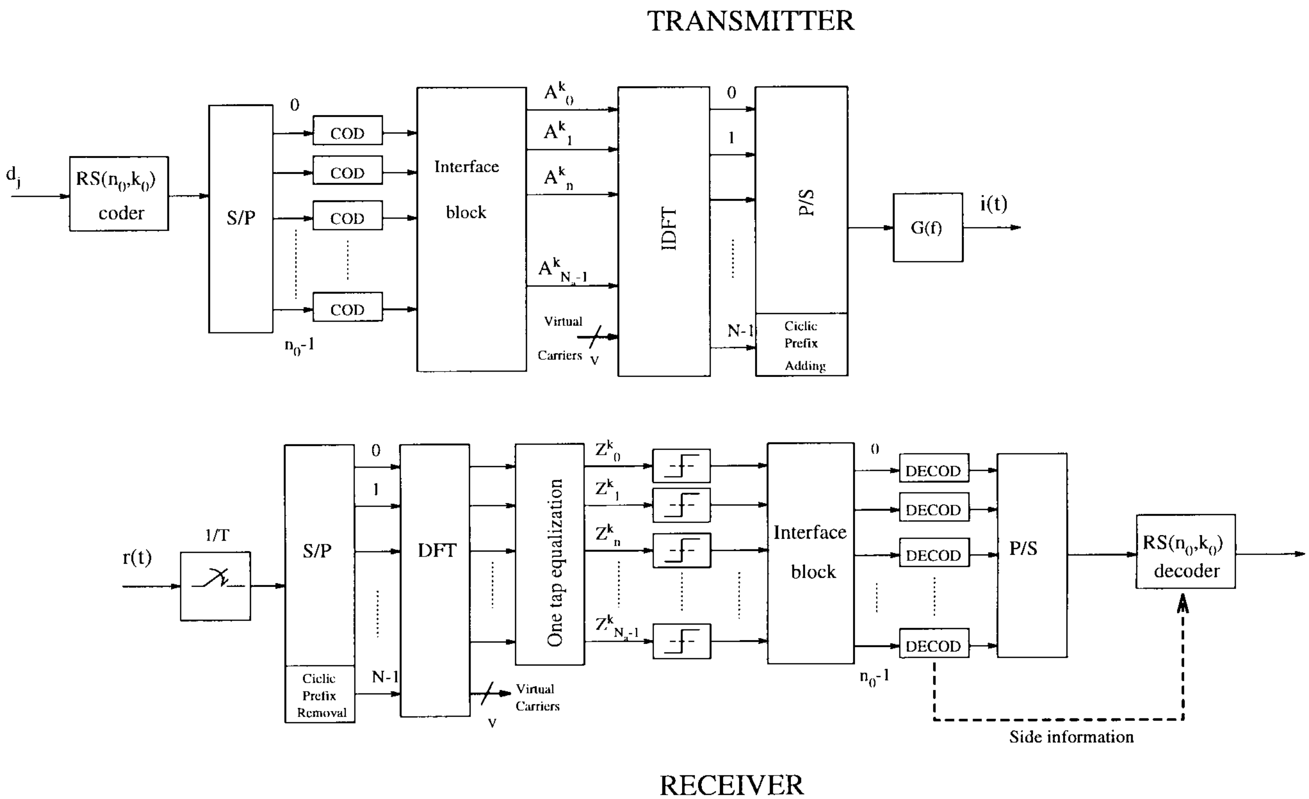

Fig. 12. Coded OFDM system block scheme.

that aliasing effects due to filtering are avoided. Thus, the OFDM modulator works with a total of $N = N_a + V$ subcarriers.

Reed–Solomon codes and their shortened versions [66] with hard-decision decoding are considered. These are nonbinary codes built with symbols composed of m_o bits; their natural length is $n_o = 2^{m_o} - 1$. As they have minimum distance $d_m = n_o - k_o + 1$, the decoder is able to correct e erasures and c errors if $e + 2c < d_m$ $(2c < d_m$ for error correction decoding). The erasure correction capability of the decoder could be exploited by means of an inner layer of coding, as has been proposed in [88] and utilized in [7]. In this case, each of the n_o information streams is coded by means of a binary (n_i, k_i) block code—i.e., Bose–Chaudhuri–Hocquenghem code or a parity check code—to form a concatenated code with code rate $R_c = k_o k_i / n_o n_i$. In the absence of inner coding, the code rate is simply $R_c = k_o / n_o$. The inner code is mainly used for error detection in order to assure a sufficiently reliable erasure detection mechanism.

At the nth input of the OFDM modulator, $n = 0, \cdots, N - 1$, each group of $\log_2 M$ bits is mapped to a complex symbol of an M-ary constellation leading to a frame of N complex symbols at the kth discrete instant and to an M-QAM signaling. The symbol duration at each channel is given by

$$T_s = \frac{\log_2 M \xi_V N R_c}{B_r} \tag{27}$$

where

$$\xi_V = \frac{N - V}{N}. \tag{28}$$

At the output of the inverse DFT block, we obtain a vector of N samples $U_i^k = \mathcal{F}_d^{-1}[A_n^k]$ for $i = 0, \cdots, N-1$, where $\mathcal{F}_d$ is the DFT. This output is parallel-to-serial converted to a sample stream with chip time T, which is then transmitted by means of a quadrature modulator. To eliminate the effects of channel distortion caused by multipath propagation, a guard interval T_g approaching the maximum delay of the propagation channel is introduced. During the guard time, a cyclic prefix sequence with integer length $D = T_g / T$ has to be transmitted. The chip time becomes $T = T_s / N + D$, and the spectrum efficiency is reduced by a factor

$$\xi_D = \frac{N}{N + D}. \tag{29}$$

The complex envelope of the signal at the output of the transmitter $i(t)$ is obtained by using a suitable bandlimited pulse with Fourier transform $G(f)$. The signal obtained here by means of a DMT technique corresponds to a multicarrier OFDM signal where, due to orthogonality, the different subcarriers are spaced $\Delta f = 1/NT$. The total bandwidth required is assumed to be $B_c = N \Delta f$, leading to

$$B_c = \frac{B_r}{\log_2 M \xi_D \xi_V R_c}. \tag{30}$$

At the receiver side, the demodulated signal is sampled at rate $1/T$. After serial-to-parallel conversion, the first D

samples are removed (cyclic prefix), and the remaining N complex samples are passed to the DFT block. The function $R(f) = G(f)F_{r_0}(f)$ is assumed to be a raised cosine function with rolloff factor α, and the low-pass transfer function of the receiving filter $F_{r_0}(f)$ is assumed to be matched with $G(f)$. By assuming ideal frequency and time synchronisms and perfect channel parameter estimation, we have the decision variables Z_n^k at the input of decision devices depending on the samples of H_n.

The bits at the output of the OFDM modulator feed the inner and outer decoders, which try to regenerate the transmitted message. Inner decoders also provide erasure detection to improve the efficiency of the outer decoder.

ACKNOWLEDGMENT

The authors wish to thank M. Chiani, D. Dardari, G. Mazzini, and A. Vaccari for useful discussions in developing this work.

REFERENCES

[1] M. Nakagawa and L. Michael, "Wireless communication technology in intelligent transport systems," in *Wireless Communications: TDMA Versus CDMA*, S. G. Glisic and P. A. Leppanen, Eds. Norwell, MA: Kluwer, 1997, pp. 491–508.

[2] O. Andrisano, "Short range 60 GHz communication systems for vehicle applications," presented at the DACAR Steering Committee Meeting, Munich, Jan. 1991.

[3] O. Andrisano, M. Chiani, M. Frullone, C. Moss, and V. Tralli, "Millimeter wave short range communications for advanced transport telematics," *Eur. Trans. Telecommun.*, vol. 4, pp. 15–26, July–Aug. 1993.

[4] R. Verdone, "Communication systems at millimeter waves for ITS applications," presented at the IEEE Vehicular Technology Conf. (VTC'97), Phoenix, AZ, May 1997.

[5] G. McGibney, A. Sesay, J. McRory, and B. Morris, "Implementation of a high performance wireless LAN," in *Proc. ICUPC 94*, San Diego, CA, Oct. 1994, pp. 645–650.

[6] A. Chini, M. S. El-Tanany, and S. A. Mahmoud, "Transmission of high rate ATM packets over indoor radio channels," *IEEE J. Select. Areas Commun.*, vol. 14, pp. 469–476, Apr. 1996.

[7] D. Dardari and V. Tralli, "High-speed indoor wireless COFDM systems at 60 GHz: Performance and design criteria," in *Proc. IEEE GLOBECOM '97*, Phoenix, AZ, Nov. 1997, pp. 1306–1311.

[8] G. M. Stamatelos and D. D. Falconer, "Millimeter radio access to multimedia services via LMDS," *IEEE GLOBECOM '96*, London, UK, Nov. 1996.

[9] V. Tralli, A. Vaccari, R. Verdone, and O. Andrisano, "Last mile wireless broadband access to interactive services at millimeter waves," presented at the 9th Tyrrhenian International Workshop on Digital Communications, Lerici, Italy, Sept. 7–10, 1997.

[10] H. Sari, "An overview of digital MMDS and LMDS, and the technical challenges in receiver design," presented at the 9th Tyrrhenian International Workshop on Digital Communications, Lerici, Italy, Sept. 7–10, 1997.

[11] G. Coppola, "42 GHz broadband wireless access to interactive services," presented at the 9th Tyrrhenian International Workshop on Digital Communications, Lerici, Italy, Sept. 7–10, 1997.

[12] L. Noel, L. D. Westbrook, D. G. Moodie, and D. Nesset, "120 Mbit/s QPSK data and multi-channel TV transmission over 13 Km fiber to a 60 GHz mobile radio link using an electroabsorption modulator as a transceiver," *Electron. Lett.*, vol. 33, no. 15, pp. 1285–1286, July 17, 1997.

[13] A. Plattner, "60 GHz mobile communications, propagation and technology requirements," presented at the 23rd Eur. Microwave Conf. (EuMC'93), Workshop on Mobile Communications, Madrid, Spain, Sept. 1993.

[14] P. F. M. Smulders and A. G. Wagemans, "Wideband indoor radio propagation measurements at 58 GHz," *Electron. Lett.*, vol. 28, no. 13, pp. 1270–1272, June 1992.

[15] A. M. Hammoudeh and G. Allen, "Millimetric wavelengths radiowave propagation for line-of-sight indoor microcellular mobile communications," *IEEE Trans. Veh. Technol.*, vol. 44, pp. 449–460, Aug. 1995.

[16] T. Ihara, T. Manabe, M. Fujita, T. Matsui, and Y. Sugimoto, "Research activities on millimeter-wave indoor wireless communications systems at CRL," in *Proc. ICUPC'95*, Tokyo, Japan, Nov. 1995, pp. 197–200.

[17] T. Manabe, K. Sato, H. Masuzawa, K. Taira, T. Ihara, Y. Kasashima, and K. Yamaki, "Polarization dependence of multipath propagation and high-speed transmission characteristics of indoor millimeter-wave channel at 60 GHz," *IEEE Trans. Veh. Technol.*, vol. 44, pp. 268–273, May 1995.

[18] T. Manabe, Y. Miura, and T. Ihara, "Effects of antenna directivity and polarization on indoor multipath propagation characteristics at 60 GHz," *IEEE J. Select. Areas Commun.*, vol. 14, pp. 441–448, Apr. 1996.

[19] P. Marinier, G. Y. Delisle, and L. Talbi, "A coverage prediction technique for indoor wireless millimeter waves systems," *Wireless Personal Commun.*, vol. 3, pp. 257–271, 1996.

[20] S. Guerin, "Indoor wideband and narrowband propagation measurements around 60.5 GHz in an empty and furnished room," in *Proc. VTC'96*, Atlanta, GA, 1996, pp. 160–164.

[21] L. M. Correia and P. O. Frances "Transmission and isolation of signal in buildings at 60 GHz," in *Proc. PIMRC'95*, Toronto, Ont., Canada, Sept. 1995, pp. 1031–1034.

[22] D. Dardari, L. Minelli, V. Tralli, and O. Andrisano "Wideband indoor communication channel at 60 GHz," in *Proc. PIMRC'96*, Taipei, Taiwan, Oct. 1996, pp. 791–794.

[23] ——, "Fast ray-tracing characterization of indoor propagation channels at 60 GHz," in *Proc. VTC'97*, Phoenix, AZ, May 1997, pp. 989–993.

[24] L. Correia and G. Lovnes, "Outdoor propagation for mobile broadband systems," presented at the 24th Eur. Microwave Conf. (EuMC'94), Short Range Communications Workshop, Cannes, France, Sept. 1994.

[25] O. Andrisano, P. Daniele, M. Frullone, and R. Verdone, "Roadside to vehicle communications at 60 GHz," presented at the 24th Eur. Microwave Conf. (EuMC'94), Cannes, France, Sept. 1994.

[26] H. Bischl, E. Lutz, and W. Shafer, "The PROMETHEUS 60 GHz channel-fading statistics and simulated packet error rates," presented at the PROMETHEUS Workshop, Monaco, Oct. 1991.

[27] W. Schafer, "Channel modeling of short range radio links at 60 GHz for mobile intervehicle communication," presented at the IEEE Vehicular Technology Conf. (VTC'91), St. Louis, MO, May 1991.

[28] L. Correia and P. Frances, "A propagation model for the estimation of the average received power in an outdoor environment in the millimeter waveband," presented at the IEEE Vehicular Technology Conf. (VTC'94), Stockholm, Sweden, June 7–10, 1994.

[29] V. Tralli and R. Verdone, "Bit error and outage probability for digital cellular systems with a small number of interferers," presented at the IEEE Pers. Ind. Mobile Radio Communications Conf. (PIMRC'96), Taiwan, Oct. 15–18, 1996.

[30] ——, "Outage domains for digital transmission systems with cochannel interference and fading," in *Proc. IEEE Int. Conf. Universal Personal Communications (ICUPC'97)*, San Diego, CA, Oct. 12–16, 1997, pp. 577–582.

[31] ——, "Performance characterization of digital transmission systems with cochannel interference," *IEEE Trans. Veh. Technol.*, to be published.

[32] M. Chiani, "Analytical distribution of linearly-modulated cochannel interferers," *IEEE Trans. Commun.*, vol. 45, pp. 73–79, Jan. 1997.

[33] "Special section on ITS," *IEEE Commun. Mag.*, vol. 34, Oct. 1996.

[34] "Special issue on intelligent vehicle highway systems," *IEEE Trans. Veh. Technol.*, vol. 40, Feb. 1991.

[35] W. Kremer, D. Hubner, S. Hoff, T. P. Benz, and W. Shafer, "Computer-aided design and evaluation of mobile radio local area networks in RTI/IVHS environments," *IEEE J. Select. Areas Commun.*, vol. 11, pp. 406–421, Apr. 1993.

[36] R. Hager, R. Mathar, and J. Mattfeldt, "Intelligent cruise control and reliable communication of mobile stations," *IEEE Trans. Veh. Technol.*, vol. 44, pp. 443–448, Aug. 1995.
[37] W. Kremer and W. Kremer, "Vehicle density and communication load estimation in mobile radio local area networks (MR-LAN's)" presented at the IEEE Veh. Technol. Conf. (VTC'92), Denver, CO, May 1992.
[38] J. Kaltwasser and J. Kassubek, "A new cooperative optimized channel access for inter-vehicle communication," presented at the Vehicle Nav. Information Systems Conf. (VNIS'94), Yokohama, Japan, Sept. 1994.
[39] O. Andrisano, M. Chiani, V. Tralli, and R. Verdone, "Impact of cochannel interference on vehicle to vehicle communications at millimeter waves," presented at the IEEE Int. Conf. Communication Systems (ICCS'92), Singapore, Nov. 1992.
[40] O. Andrisano, D. Dardari, and R. Verdone, "Code division and time division multiple access networks for vehicle-to-vehicle communications at 60 GHz," presented at the IEEE Vehicular Technology Conf. (VTC'94), Stockholm, Sweden, June 7–10, 1994.
[41] R. Verdone, "Time and frequency selectivity effects in vehicle-to-vehicle communications at 60 GHz," IEEE Vehicular Technology Conf. (VTC'94), Stockholm, Sweden, June 7–10, 1994.
[42] ——, "Outage probability analysis for short range communication systems at 60 GHz in ATT urban environments," *IEEE Trans. Veh. Technol.*, vol. 46, pp. 1027, 1039, Nov. 1997.
[43] ——, "Multi-hop R-aloha for inter-vehicle communications at millimeter waves," *IEEE Trans. Veh. Technol.*, vol. 46, pp. 992–1005, Nov. 1997.
[44] K. Pahlavan, T. H. Probert, and M. E. Chase "Trends in local wireless networks," *IEEE Commun. Mag.*, vol. 33, pp. 88–95, Mar. 1995.
[45] R. O. LaMarie, A. Krishna, P. Bhagwat, and J. Panian, "Wireless LAN's and mobile networking: Standard and future directions," *IEEE Commun. Mag.*, vol. 34, pp. 86–94, Aug. 1996
[46] A. Falsafi, K. Pahlavan, and G. Yang, "Transmission techniques for radio LAN's—A comparative performance evaluation using ray tracing," *IEEE J. Select. Areas Commun.*, vol. 14, pp. 477–491, Apr. 1996.
[47] T. Wilkinson, T. Phipps, and S. K. Barton, "A report on HIPERLAN standardization," *Int. J. Wireless Inform. Networks*, vol. 2, pp. 99–120, Mar. 1995.
[48] E. Ayanoglu, K. Y. Eng, and M. J. Karol "Wireless ATM: Limits, challenges, and proposals," *IEEE Personal Commun. Mag.*, vol. 3, pp. 18–34, Aug. 1996.
[49] D. Falconer, "A system architecture for broadband millimeter-wave access to an ATM LAN," *IEEE Personal Commun. Mag.*, vol. 3, pp. 36–41, Aug. 1996.
[50] L. J. Cimini, B. Daneshrad, and N. R. Sollenberger, "Clustered OFDM with transmitter diversity and coding," in *Proc. GLOBECOM'96*, London, UK, Nov. 1996, pp. 703–707.
[51] S. Ariyavisitakul and L. J. Greenstein, "Reduced-complexity equalization techniques for broadband wireless channels," *IEEE J. Select. Areas Commun.*, vol. 15, pp. 5–15, Jan. 1997.
[52] J. R. Jones, "Baseband and passband transport systems for interactive video services," *IEEE Commun. Mag.*, pp. 90–101, May 1994.
[53] W. Honcharenko, J. P. Kruys, D. Y. Lee, and N. J. Shah, "Broadband wireless access," *IEEE Commun. Mag.*, pp. 20–26, Jan. 1997.
[54] J. G. Proakis, *Digital Communications*, 3rd ed. New York: McGraw-Hill, 1995.
[55] T. S. Rappaport, *Wireless Communications.* Englewood Cliffs, NJ: Prentice-Hall, 1996.
[56] W. C. Jakes, *Microwave Mobile Communications.* New York: Wiley, 1974.
[57] R. W. Chang, "Synthesis of band-limited orthogonal signals for multichannel data transmission," *Bell Syst. Tech. J.*, vol. 45, pp. 1775–1796, Dec. 1966.
[58] B. R. Saltzberg, "Performance of an efficient parallel data transmission system," *IEEE Trans. Commun.*, vol. COM-15, pp. 815–811, Dec. 1967.
[59] S. B. Weinstein and P. M. Ebert, "Data transmission by frequency division multiplexing using the discrete Fourier transform," *IEEE Trans. Commun.*, vol. COM-19, pp. 73–83, Oct. 1971.
[60] L. J. Cimini, "Analysis and simulation of a digital mobile channel using orthogonal frequency division multiplexing," *IEEE Trans. Commun.*, vol. COM-33, pp. 665–775, July 1985.
[61] B. Le Floch, R. Halbert, and D. Castelain, "Digital sound broadcasting to mobile receivers," *IEEE Trans. Consumer Electron.*, vol. 35, pp. 493–503, Aug. 1989.
[62] J. S. Chow, J. C. Tu, and J. M. Cioffi, "A discrete multitone transceiver system for HDSL applications," *IEEE J. Select. Areas Commun.*, vol. 9, pp. 895–908, Aug. 1991.
[63] T. Pollet, M. Van Bladel, and M. Moeneclay, "BER sensitivity of OFDM systems to carrier frequency offset and Wiener phase noise," *IEEE Trans. Commun.*, vol. 43, no. 2/3/4, pp. 191–193, Feb./Mar./Apr. 1995.
[64] T. A. Wilkinson and A. E. Jones, "Minimization of the peak to mean envelope power ratio of multicarrier transmission schemes by block coding," in *Proc. VTC'95*, Chicago, IL, July 1995, pp. 825–829.
[65] S. H. Muller and J. B. Huber, "A comparison of peak power reduction schemes for OFDM," presented at IEEE GLOBECOM '97, Phoenix, AZ, Nov. 1997.
[66] S. Lin and D. J. Costello, *Error Control Coding: Fundamentals and Applications.* Englewood Cliffs, NJ: Prentice-Hall, 1983.
[67] V. Tralli, A. Vaccari, R. Verdone, and O. Andrisano, "Adaptive C-OFDM system at 30 GHz for the last mile wireless broadband access to interactive services," IEEE ICC'98, to be presented.
[68] M. C. Lawton and J. P. McGeehan, "The application of a deterministic ray launching algorithm for the prediction of radio channel characteristics in small-cell environment," *IEEE Trans. Veh. Technol.*, vol. 43, pp. 955–969, Nov. 1994.
[69] P. Vasconcelos and L. M. Correia, "Fading characterization of the mobile radio channel at the millimeter waveband," presented at IEEE VTC'97, Phoenix, AZ, May 5–7, 1997.
[70] D. Dardari and V. Tralli, "High-speed indoor wireless communications at 60 GHz with coded OFDM," Tech. Rep. CSITE001-97, Mar. 1997, submitted for publication.
[71] R. Prasad and B. C. van Lieshout, "Cochannel interference probability for micro- and picocellular systems at 60 GHz," *Electron. Lett.*, vol. 29, pp. 1909–1910, Oct. 1993.
[72] Y. S. Yeh and S. C. Schwartz, "Outage probability in mobile telefony due to multiple log-normal interferers," *IEEE Trans. Commun.*, vol. COM-32, pp. 380–388, Apr. 1984.
[73] K. W. Sowerby and A. G. Williamson, "Outage probability calculations for multiple cochannel interferers in cellular mobile radio systems," *Proc. Inst. Elect. Eng.*, vol. 135, pp. 208–215, June 1988.
[74] Y.-D. Yao and A. U. H. Sheikh, "Outage probability analysis for microcellular mobile radio systems with cochannel interferers in Rician/Rayleigh fading environment," *Electron. Lett.*, vol. 26, pp. 864–866, 1990.
[75] G. L. Stuber and L. B. Yiin, "Downlink outage predictions for cellular radio systems," *IEEE Trans. Veh. Technol.*, vol. 40, pp. 521–531, 1991.
[76] R. Prasad, A. Kegel, and M. B. Loog, "Cochannel interference probability for picocellular systems with multiple Rician faded interferers," *Electron. Lett.*, vol. 28, pp. 2225–2226, Nov. 1992.
[77] A. A. Abu-Dayya and N. C. Beaulieu, "Outage probabilities of diversity cellular systems with cochannel interference in Nakagami fading," *IEEE Trans. Veh. Technol.*, vol. 41, pp. 343–355, Nov. 1992.
[78] M. Chiani, V. Tralli, and R. Verdone, "Outage and spectrum efficiency analysis in microcellular systems," presented at the IEEE Vehicular Technology Conf. (VTC'93), Secaucus, NJ, May 18–20, 1993.
[79] G. Mazzini and R. Verdone, "Semi-analytical evaluation of outage probability for Pico and microcellular mobile radio systems with correlated shadowing," *Electron. Lett.*, vol. 29, no. 13, pp. 1214–1215, June 24, 1993.
[80] H. D. M. Gurr, K. W. Sowerby, and A. G. Williamson, "Generalized outage probability and BER estimation using dual protection margins," presented at the IEEE Vehicular Technology Conf. (VTC'94), Stockholm, Sweden, June 7–10, 1994.
[81] D. Dardari, "A general approach to the evaluation and characterization of packet radio networks performance," *Int. J. Wireless Inform. Net.*, vol. 3, no. 4, pp. 203–217, Oct. 1996.
[82] R. Verdone, "Joint effects of co-channel interference, fading, shadowing and noise on outage probability," *Electron. Lett.*, vol. 32, no. 5, pp. 428–429, Feb. 29, 1996.
[83] N. Abramson, *Multiple Access Communications.* New York: IEEE Press, 1993.

[84] J. C. Arnbak and W. Blitterswijk, "Capacity of slotted ALOHA in Rayleigh-Fading channels," *IEEE J. Select. Areas Commun.*, vol. SAC-5, pp. 261–269, Feb. 1987.
[85] T. Liu, J. A. Sylvester, and A. Polydoros, "Performance evaluation of R-ALOHA in distributed packet radio networks with hard real-time communications," presented at the IEEE Vehicular Technology Conf. (VTC'95), Chicago, IL, July 25–28, 1995.
[86] O. Andrisano, D. Dardari, and G. Mazzini, "An integrated approach for the design of wide-band wireless LAN," ICT'98, to be presented.
[87] J. Roberts and T. Healey, "Packet radio performance over Rayleigh fading channels," *IEEE Trans. Commun.*, vol. COM-28, pp. 279–286, Feb. 1980.
[88] A. M. Saleh and L. J. Cimini, "Indoor radio communications using time-division multiple access with cyclical slow frequency hopping and coding," *IEEE J. Select. Areas Commun.*, vol. 7, pp. 59–70, Jan. 1989.

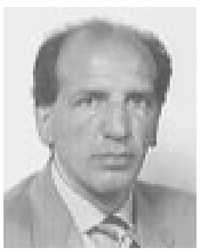

Oreste Andrisano (Member, IEEE) was born in Bologna, Italy, on February 14, 1952. He received the Dr.Ing. degree in electronic engineering (*cum laude*) from the University of Bologna in 1975.

That year, he joined the University of Bologna, where he became a Professor of electrical engineering in 1985 and Director of the Centro di Studio per l'Informatica e i Sistemi di Telecomunicazioni—Consiglio Nazionale delle Richerche in 1993. His research activity has been concerned with different fields in the digital communication area such as digital signal processing, data transmission for satellite and fixed radio links applications, local wireless, and mobile radio networks. In 1987 and 1988, he cooperated in the definition phase of two European research programs, PROMETHEUS (EUREKA) and DRIVE (ECC), which were oriented to the implementation of a sophisticated mobile communications network to make road traffic safer, more economical, and more efficient. He also worked as an Italian representative within the Steering Committee of the European research program DRIVE/DACAR as a member of the coordination group. He then was the National Coordinator of the PROCOM/PROMETHEUS and Telecommunication Networks for Cooperative Driving (TELCO) research activities.

Dr. Andrisano is a member of the Italian Electrotechnical and Electronic Association. He is a member of the IEEE Communication and Vehicular Technology Societies and of the IEEE Radiocommunication Committee. He is an Editor of IEEE TRANSACTIONS ON COMMUNICATIONS for "Modulation for fading channels."

Velio Tralli (Member, IEEE) was born in Carpi, Italy, on April 14, 1964. He received the Dr.Ing. degree (with honors) in electronic engineering and the Ph.D. degree from the University of Bologna, Bologna, Italy, in 1989 and 1993, respectively.

He began his research activity in the Department of Electronics, Computer Science and Systems, University of Bologna. In 1994, he joined the Centro di Studio per l'Informatica e i Sistemi di Telecomunicazioni at the University of Bologna, where he is currently developing its activity as a Researcher of the Consiglio Nazionale delle Richerche. Since 1994, he has also been a Lecturer of digital communications at the University of Ferrara, Ferrara, Italy. His research interests are in the area of wireless communications systems, with emphasis on broad-band indoor and outdoor wireless systems, spread-spectrum communications systems, and digital cellular systems. He was involved in the European research program PROMETHEUS.

Roberto Verdone (Member, IEEE) was born in Bologna, Italy, on August 6, 1965. He received the Dr.Ing. degree in electronic engineering (with honors) and the Ph.D. degree in electronic engineering and computer science from the University of Bologna, Bologna, Italy, in 1991 and 1995, respectively.

Since 1996, he has been a Researcher with the Centro di Studio per l'Informatica e i Sistemi di Telecomunicazioni—Consiglio Nazionale delle Richerche, Bologna. Since 1994, he has been a Lecturer on telecommunication systems and digital transmission at the University of Bologna. Since 1997, he has been a Lecturer on digital transmission at the University of Ferrara, Ferrara, Italy. His research activity is concerned with digital modulation, interference control, cellular and mobile systems, handover techniques, multiple access, and spectrum efficiency. Part of his work is dedicated to intervehicle and vehicle-to-infrastructure communications at millimeter waves. He is also interested in the analysis of digital broadcasting systems. In 1992, he was involved in the European research program PROMETHEUS. Since 1997, his work has also been conducted in the context of COST 259 activities.